

## Chapter II

### Theory

#### 2.1 Silica Powders

Silica powder may consist of small granules of silica gel or of coherent aggregates of submicron particles that are linked together in extremely weak networks. Theoretically, a silica powder might consist of separate, discrete silica particles, but when the particle diameter is less than 100 nm, the particles spontaneously adhere together in loose aggregates. There are silicas which are on the borderline between a gel and a powder. When the bonds between the ultimate colloidal particles are very weak, and can be readily broken by mechanical means, the silica can be classed as a powder. On the other hand, when the colloidal particles form a strong, coherent structure, the silica is classed as a gel even though the size of the gel granules may be as small as a few micron.

##### 2.1.1 Types of Powders

Silica powders can be classified according to the way in which they have been made, which usually confers special characteristics.

Pulverized gels are made by grinding of xerogels. Ultimate gel structure remain unchanged.

Spheroidal gels are made by subdividing the precursor silicic acid or colloidal sol into fine droplets before gelling. The gel structure is similar to gels formed under the same conditions. The droplets may be suspended in air and dried or may be suspended in an immiscible liquid in which the droplets solidify. The droplets may also be formed in an aqueous phase by coacervation of colloidal silica with an organic agent to form droplets which are then solidified.

Precipitated silica is formed when the ultimate silica particles are coagulated as loose aggregates in the aqueous medium, recovered, washed, and dried. Coagulation may be effected by high salt concentration or other coagulants such as ammonia, water miscible solvents, or certain types of organic materials. When the ultimate particles are larger than 5-10 nm, they may be only weakly joined together and if in an open-packed condition subsequently they can easily be broken apart and dispersed, for example, in oils of rubber.

Aerosils or pyrogenic silica are powders made by condensing silica from the vapor phase at elevated temperature. The silica vapor is produced by (a) direct volatilization of  $\text{SiO}_2$ , (b) reduction of  $\text{SiO}_2$  to volatile  $\text{SiO}$  which is reoxidized, (c) oxidation of volatile silicon compounds such as chloride or esters, or (d) vapor phase hydrolysis of  $\text{SiF}_4$ .

Organophillic silicas are made from all the foregoing types of powders by covering the surface with a monomolecular chemisorbed layer of organic groups attached to the surface atom through  $\equiv\text{Si-C}$ ,  $\equiv\text{Si-O-C}$ ,  $\equiv\text{Si-O-N}^+\text{-C}$ ,  $\equiv\text{Si-O-M-O-C}$  types of linkages (M is a polyvalent metal cation).

### 2.1.2 Physical Characterization

Most of the methods of characterization apply to powders. (Buzargh, 1937) identified the variables that must be taken into account to define an aggregate structure.

1. the size and shape of the primary particles;
2. the spatial distribution of the particles, including the order and density of packing;
3. the strength of the bond between particles (coalescence);

In powders, the ultimate or primary particles are always aggregated into what has been termed "secondary particles", "clusters", or "aggregate particles". For convenience, therefore, different silica particles may be defined as follows :

Primary particles : 1.5 nm to 2.5 (i.e., 2000 to 7500 molecular weight) silica particles.

Secondary particles : High co-ordinate number aggregate of the primaries. Typically 8.0 - 50.0 nm diameter.

Tertiary particles : Low co-ordination number aggregates, typically in the micron-size range.

Higher aggregates due to gel formation (ground xerogels)

## 2.2 Sol-Gel Processing

### 2.2.1 General Sol-Gel Processing

Alkoxide sol-gel processing (see figure 2.1) is a chemical synthesis of oxides involving hydrolyzable alkoxides that undergo a sol-gel transition. Sol-gel processing in general refers to any system that undergoes a sol-gel transition, including colloidal sols and soluble salts.

Sol-gel processing has been used to prepare glasses, glass-ceramics, and ceramics. Either amorphous or crystalline materials can result depending on the composition, the precursors, the handling, and heat treatment. These factors lead to either a powder process (that uses discrete particles) or a powder-free process (any process that does not involve an aggregation of discrete particles). Starting from hydrolyzable alkoxides, a powder-free process would generate a porous preform of a glass or ceramic in the desired geometry by linking molecular species directly. The desired geometry may be a thin film, a fiber, or a bulk shape called a monolith. Whether sol-gel processing is carried out as a powder process or as a powder-free process, one of the reasons for application is the purity of the starting materials.

The process involving sols which are colloidal dispersions is defined as follows: A sol is a dispersion of solid particles called the disperse phase, in a liquid, called the dispersion medium, in which at least one dimension of the particles in the solid phase is between 1 nm and 1  $\mu\text{m}$  (see figure 2.2). Particles in the disperse phase contain few atoms, typically from  $10^3$  -  $10^9$  per particle. A gel is what results as the viscosity rises, e.g., by the loss of liquid, or by increased cross-linking. Silica gels are the oldest and most closely studied. Fused silica represents the most explored of bulk glasses formed by sol-gel processing. The reasons for this are that silica forms a single-component oxide glass, and here is an increasing demand for high-quality (and high - purity) fused silica optical components with high transmission in ultraviolet (UV) and infrared (IR) wavelengths. Table 2.1 shows, there are now many systems that can be gelled from suitable sols, including almost half of the periodic table.

The steps in the process, and how they give rise to the range of products from powders to monoliths, are compiled below in figure 2.3.

The first stage is the sol preparation by mixing solutions and/or colloidal suspensions. This is the gel-forming medium. Two types are distinguished, depending on the processed leading to destabilization of the sol :

(i) Alcogel : this emerges from the medium when the destabilization processes are hydrolysis and polycondensation of alkoxide solutions.

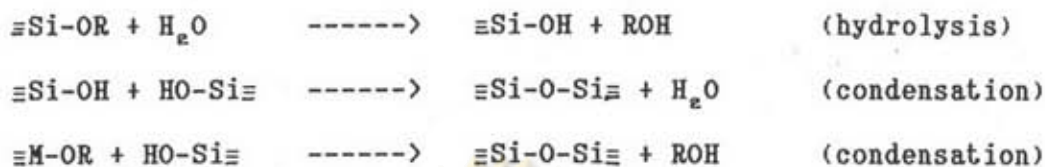
(ii) Aquagel : this is ion adsorption and occlusion of foreign cations by normally stable silica sols destabilized by electrolyte control.

Stage two in figure 2.3 is most important with respect to the form of the product, because it represents the same process occurring at vastly different rates. If excess water is used to rapidly destabilize the sol (route B in figure 2.3), a gel is produced which in the next stage leads to a powder, but if slow hydrolysis via atmospheric moisture is the route taken (A in figure 2.3), gels are produced from which fibres, monoliths and coatings can be obtained.

During stage 2, the aquagels or the alcogels become stiff materials consisting of elementary gel particles that are interconnected and contain interstitial liquid from the medium. Sol particles can be destabilized by electrolyte modification of pH and reduction of electrical repulsion between them, leading to continuous networks of separate particulate aggregates. This is sometimes referred to as "colloidal" gel to distinguish it from a "polymeric" gel formed when sol particles are increased in size by a condensation polymerization reaction from solution. Thus colloidal gels usually

stem from aquagels, and polymeric gels from alcogels.

The hydrolysis and polycondensation to silica alcogels may be summarized by the following steps :



Only the second reaction, i.e., the condensation of hydroxyl groups, occurs in aquagel condensation, binding particles together by  $\equiv\text{Si-O-Si}\equiv$  bridges.

Stage 3 in the overall process is the removal of the interstitial dispersion medium, during which process the solid also shrinks to give a porous solid known as xerogel.

### 2.2.2 Factors Controlling Gel Characteristics

The final characteristics of a finished, dried gel are determined by the physical and chemical conditions at every step of the process of preparation. These are :

the size of the primary silica particles at the moment they aggregate into the gel network;

the concentration of the primary particles in solution and thus the compactness of the gel network;

the pH, salt concentration, temperature, and time during which the gel is aged or otherwise treated while in the wet state (this includes the possible step of replacing water with a water-miscible liquid like alcohol);

mechanical pressure or shearing forces applied to the gel before or during drying;

condition of temperature, pressure, pH, and salt content, and surface tension of the liquid medium as being evaporated from

the pores of the gel;

temperature, time, and type of atmosphere in which the gel is heated after being dried.

### 2.2.3 Advantages and Limitations of the Sol-Gel Process

The advantages of the sol-gel process in general are high purity, homogeneity, and low temperature. Because the precursors can be distilled and filtered, the products are relatively free of impurities. Because the mixing is accomplished in solution, components mix on the nanometer scale in relatively short times. If the intention to use this processes is to make a dense material, the porous dried gel can be compacted at temperatures one-third (to one-half) lower than the liquidus temperature in K. For silica, this means 1050°C vs 1723°C

For a lower temperature process, there is a reduced loss of volatile components. In fact, some compositions that cannot be made by conventional means because of phase separation or devitrification. In some systems, the sol-gel process extends the glass-forming range.

One of the primary advantages of the sol-gel process, especially in the form of films, is that the material is used efficiently. Any excess material is recovered and can be used again.

### 2.2.4 Disadvantages of the Sol-Gel Process

2.2.4.1 The colloidal gel monoliths have very small pore structures and relatively low densities. Removal of the solvents from these open networks and the overall shrinkage in processing require special techniques to avoid cracking. In addition, thermal processing must take into account high surface water and carbonaceous residues that can lead to bloating, residual bubbles, or crystal formation if not properly removed. These barriers tend to limit the size of

monolithic glass parts that can be produced by direct casting procedures.

2.2.4.2 The high-purity alkoxides are relatively expensive raw materials.

2.2.4.3 Multi-step processing adds time and expense. It is unlikely that high-volume glass products, such as containers, cooking ware, flat glass and common fiber, would be produced economically by sol-gel technologies, which have found their rich in the specialty products area.

## 2.2.5 Sols

### 2.2.5.1 Primary particles

The solubility,  $C$ , of a particle is related to its size by the Gibbs free energy of dissolution  $G$ . For the dissolution of a single particle with diameter  $d$ , we have the particle-related Gibbs free energy

$$\Delta G(\text{particle}) = \Delta G_{\infty} - \pi d^2 \cdot \sigma \quad **$$

$\Delta G_{\infty}$  = value for the infinitely extended phase

$\sigma$  = interfacial tension between solid and liquid

\*\*Note : The action of the interfacial tension makes dissolution more likely, hence the minus sign.

Multiplying this equation by  $M/((\pi/6)d^3 \rho)$  converts the  $G$  into a molar quantity yielding

$$\Delta \bar{G} = \Delta \bar{G}_{\infty} - 6\sigma M/(d \cdot \rho)$$

$M$  = Molar mass in g/mol

$\rho$  = density in g/cm<sup>3</sup>

With the saturation concentration of the infinitely extended phase ( $d \rightarrow \infty$ ) given as



$$C_0 = \exp(-\bar{\Delta G}_0/R.T)$$

we can formulate the saturation concentration of a colloidal particle as

$$C = \exp(-\bar{\Delta G}/R.T) = C_0 \cdot \exp(6\sigma M/R.T.d.)$$

This is also known as the Ostwald - Freundlich equation. It is illustrated for silica in figure 2.4. The effect of size on solubility is most important for particles with diameter < 5 nm; smaller particles in this size range will tend to dissolve and reprecipitate on larger particles. This process of particle growth, known as Ostwald ripening, will raise the average diameter of the silica particles to 5 to 10 nm at pH > 7, whereas at low pH growth will be negligible for particles larger than 2 to 4 nm. The final particle sizes increase with temperature and pressure, as both factors increase the solubility of silica. Since the condensation reaction is exothermic, each Si atom tries to surround itself with four siloxane (i.e.,  $\equiv\text{Si-O-Si}\equiv$ ) bonds. For particles smaller than 5 nm, more than 50% of the Si atoms are on the surface, so they must have one or more silanol (i.e.,  $\equiv\text{Si-OH}$ ) bonds; nevertheless, the interior of the colloidal particles can be regarded as dense  $\text{SiO}_2$ .

#### 2.2.5.2 Stability of sols

The stability and coagulation of sols is the most intensively studied aspect of colloidal chemistry. Since the electrons surrounding a nucleus do not constitute a spatially and temporally uniform screen, every atom is a fluctuating dipole. This effect creates an attraction between atoms known as the van-der-Waals force or dispersion energy, which is proportional to the polarizabilities of the atoms and inversely proportional to the sixth power of their distance. The van-der-Waals forces result from three types of

interactions : permanent dipole - permanent dipole (Keesom forces), permanent dipole-induced dipole (Debye forces), and transitory dipole-transitory dipole (London forces). It is the London forces that produce the long-range attraction between colloidal particles (see figure 2.5). When atoms are far apart, the movement of their electrons will distribute so as to minimize the energy of the system.

The stabilization of colloids by electrostatic repulsion is successfully described by the DLVO theory (named after its principal creators, Derjaguin, Landau, Verwey, and Overback). The net force between particles in suspension is assumed to be the sum of attractive van-der-Waals forces and the electrostatic repulsion created by charged adsorbed on the particles. The repulsive barrier depends on two types of ions that make up the so-called double layer : charge-determining ions that control the charge on the surface of the particles and counterions that are in solution in the vicinity of the particles and act to screen the charges of the potential determining ions. For hydrous oxides, the charge-determining ions are  $H^+$  and  $OH^-$ , which establish the charge on the particle by protonating or deprotonating the MOH bonds on the surfaces of the particles ;



The ease by which protons are added or removed from the oxide (that is to say the acidity of the MOH group) depends on the metal atom. The pH at which the particle is neutrally charged is called the point of zero charge (PZC). At  $pH > PZC$ , the second reaction predominates, and the particle is negatively charged, whereas at  $pH < PZC$ , the first reaction gives the particle a positive charge. Values of the PZC for several oxides are given in Table 2.2 ;



the data are taken from an extensive tabulation by Parks (1965).

#### 2.2.5.3 Structure of sols

There is a strong analogy between the behavior of particles in a sol and atoms in a fluid. At low concentration, the particles behave independently, like atoms in a gas. As the concentration increases, short-range ordering appears. Further increases in concentration can lead to a cluster or gel in which the arrangement of primary particles is amorphous or crystalline. Aksay and Kikuchi (1986) have calculated phase diagrams for sols, introducing a parameter proportional to the square of the  $\zeta$ -potential, which the authors interpret as a characteristic temperature. When the "temperature"  $T \propto \zeta^2$  is high the sol is gaslike. Lowering  $T$  leads to the formation of "glasses" or "crystals". There is also a miscibility gap in which ordered clusters form and precipitate, leaving monomers in suspension. A sudden decrease in  $T$  leaves no time for ordering, so an unstructured aggregate is formed (see figure 2.6), in analogy to the formation of a glass by rapid quenching of a melt. Slow reduction in  $T$  allows ordering into a crystalline structure.

Roughly speaking, the  $\zeta$ -potential is the effective potential which is felt outside of the (diffuse) double layer. It is equal to the surface potential minus the shielding effect of attached counterions. The PZC refers to the surface potential. When the potential becomes zero, this is referred to as IEP (isoelectric point).

#### 2.2.6 Gels

The pH and electrolyte concentration determine the time  $t_{gel}$  of gel formation. At high pH the particles are stabilized by a

negative charge, so  $t_{\text{set}}$  is long, however, the effectiveness of the electrostatic barrier is sensitive to the presence of salts that compress the double layer. For most oxides, the gelation rate increases continuously as the isoelectric point is approached, but silica is anomalous : near the IEP (pH  $\sim$  2) the stability is only moderate, apparently because of protection provided by layers of bound (adsorbed) water (Iler, 1979). At lower pH ( $\ll$  IEP), where the particles become positively charged, instability is attributed to fluoride impurities.

The structure of a gel made from colloidal particles depends on the size distribution of the particles and the strength of the attractive forces between them. If the particles are spherical and monodisperse, and the repulsive barrier is reduced gradually, the sol may develop an ordered ("crystalline") structure.

### 2.3 Drying

The major problem of making bulk samples by the sol-gel process is the large volume shrinkage involved and the usual cracking of the piece. The problem arises when the surface energy solid-liquid is less than the surface energy solid-vapor. In the wet region of a gel, the gel contracts to lower the solid-liquid surface area. When the gas phase enters the gel in the dry region, the solvent tries to cover the solid-vapor interface. Meanwhile, the dry region tends to contract to lower the solid-vapor surface area.

In drying a ceramic, the reverse occurs. As water is removed, the water layers between the particles, termed the shrinkage water, decrease in thickness, allowing particles to approach one another ; hence the shrinkage. At some point, the particles will come into

contact and are not able to move further. At this point, shrinkage is terminated, and residual water remaining in the voids, termed pore water. Removal of the pore water is not accompanied by shrinkage, making this portion of drying less critical than the removal of the interparticle water. Because the drying shrinkage is related to the interparticle water layers, bodies with finer particles (and hence more surface area per unit volume) shrink more. Naturally, the extrinsic variables independent of composition contribute also to the drying process, and are used to control its

temperature : As the temperature during drying increases, the rate of evaporation of water increases.

humidity : As the atmosphere decreases in humidity, the drying rate increases. This can be summarized by the following rate equation.

$$\begin{aligned} \text{Rate} &= \frac{\text{Sh} \cdot D}{L} \times \Delta P(T) \\ &= \frac{\text{Sh} \cdot D (P_{\text{sat}}(T) - P)}{L} \end{aligned}$$

Sh = dimensionless function describing the air flow (air circulation)

L = size of the piece to be dried

P(T) = actual water partial pressure

$P_{\text{sat}}(T)$  = saturation water partial pressure at T

D = diffusion coefficient of water vapor

The fastest drying rate possible occurs therefore at high temperature (i.e. high  $P_{\text{sat}}(T)$ ) with low humidity (i.e.,  $P \rightarrow 0$ ) and large volumes of air circulation. Ware cannot, however, be dried initially with these conditions, as too quick a removal of water causes stresses in the ware which result in warping or cracking.

The process of drying of a porous material can be divided into several stages. At first the body shrinks by an amount equal to the volume of liquid that evaporates, and the liquid-vapor interface remains at the exterior surface of the body. The second stage begins when the body becomes too stiff to shrink and the liquid recedes into the interior, leaving air-filled pores near the surface. Drying of gel results in network shrinkage in response to the capillary forces that actively transport the liquid to the surface for evaporation. The very small pores cause a higher degree of shrinkage than do the larger pores. This is because the smaller pores produce significantly higher capillary forces. Another important thing during this step is the occurrence of cracks. Too fast a drying rate causes the outer surface to dry preferentially with respect to the center of the gel, setting up a gradient of moisture. A similar gradient can occur if heat is applied non-uniformly over the gel surface. Surfaces dried preferentially tend to shrink, while the other portions of the gel do not. The drier surface is therefore in tension, the moisture one in compression. These stresses can only be relieved by cracking, depending on geometry.

### 2.3.1 The Factors Affecting Stress Development

Phenomenology describes stages of drying in detail (see figure 2.7).

A. Constant rate period discusses the first stage, when the decrease in volume of the gel is equal to the volume of liquid lost by evaporation. The compliant gel network is drawn into the liquid by capillary and/or osmotic forces. This first stage of drying is called the constant rate period (CRP), because the rate of evaporation per unit area of the drying surface is independent

of time. The chemical potential,  $g$ , of the liquid in the adsorbed film is equal to that under the concave meniscus. Otherwise, the liquid would flow from one to the other to balance the potential;  $g$  is lower than for bulk liquid because of disjoining and capillary forces, so the vapor pressure ( $P_v$ ) is lower according to

$$P_v/P_o = \exp(\Delta g/R.T)$$

Where  $P_o$  is the vapor pressure of bulk liquid (i.e., over a planar liquid surface),  $R$  is the gas constant,  $T$  is the absolute temperature.

The rate of evaporation,  $r_e$  is proportional to the difference between  $P_v$  and the ambient vapor pressure.

Evaporation causes cooling of a body of liquid, but the reduced temperature leads to a lower rate of evaporation and less cooling. When equilibrium is established, the temperature of the liquid is called the wet-bulk temperature,  $T_w$ ;  $r_e$  increases as  $P_a$  decreases, so  $T_w$  decreases with the ambient humidity. The exterior surface of a drying body is at the wet-bulb temperature during the CRP.

If there were no interaction between the liquid and solid components of the gel, the liquid would evaporate from the pores leaving the network exposed, but otherwise unchanged. In reality, adsorption and capillary forces oppose exposure of the solid phase, so liquid flows from the interior to replace that which evaporates.

B. A critical point examines the end of the first stage, when shrinkage stops and cracking is most likely to occur. As the gel shrinks, the tension in the pore increases and the vapor pressure of the liquid in the pores decreases according to

$$P_v = P_o \cdot \exp(-P.M/\rho.R.T)$$

Where  $M$  is the molar mass of the liquid and  $P$  is the tensile stress in the liquid.

$$P_A < P_o \cdot \exp \left( \frac{(-2\sigma_{LV} \cdot \cos\alpha)}{\rho \cdot R \cdot T \cdot d} \right)$$

$P_A$  is the ambient vapor pressure,  $d$  is the diameter of pores,  $\alpha$  is the wetting angle between liquid and solid. At  $P_A = 0$ , shrinkage could continue until the pores collapse completely ( $d \rightarrow 0$ ). In practice, however, the network stiffens as it shrinks and at some point becomes able to withstand the capillary pressure. Shrinkage stops at this point, which can be defined in terms of the volume fraction  $1 - \epsilon$  of solid phase, expressed by the porosity  $\epsilon$  (both liquid and air-filled).

C. The first falling rate period explains the process of liquid flow through partially empty pores. When shrinkage stops, further evaporation drives the meniscus into the body as air enters the pores. The surface may become less translucent. In the first falling rate period (FRP1), the rate of evaporation decreases and the temperature of the surface rises above the wet-bulb temperature. The liquid in the pores near the surface remains in the so-called a funicular condition in figure 2.8, (this means there are continuous pathways along which a flow can occur). Most of the evaporation is still occurring at the exterior surface, and the surface remains below the ambient temperature, and the rate of evaporation is sensitive to the ambient temperature and vapor pressure. Inhomogeneity can result as the flow carries solutes toward the surface where they may precipitate. This involves coupled equations for flow and diffusion of heat, liquid and vapor, with transport coefficients that are generally dependent on temperature and concentration.

D. The second falling rate period discusses the final stage of drying, when liquid can escape only by diffusion



of its vapor to the surface. As the meniscus recedes into the body, the exterior does not become completely dry right away, because liquid continues to flow to the outside ; as long as the flux of liquid is comparable to the evaporation rate, the funicular condition is preserved. However, as the distance from the exterior to the drying front increases, the capillary pressure gradient decreases and therefore so does the flux. Eventually (if the body is thick enough) it become so slow that the liquid near the outside of the body is isolated in pockets, so flow to the surface stops and liquid is removed from the body only by diffusion of its vapor. At this stage, drying is said to enter the second falling rate period (FRP2), where evaporation occurs inside the body. The temperature of the surface approaches the ambient temperature and the rate of evaporation becomes less sensitive to external conditions (temperature, humidity, draft rate, etc.).

The pores of a gel are so small that the vapor moves by Knudsen diffusion, which means that molecules collide more frequently with the walls of the pores than with each other. The permeation rate becomes anomalously low for polar molecules, because of interaction with the solid surface. The slow diffusion of vapor through the gel results in an abrupt drop in the drying rate at the start of FRP2. The slower drying encourages instability of the drying front which may lead to transient opacity during drying.

The capillary pressure is high in the isolated pockets, but they occupy such a small volume fraction that they do not exert much force on the solid network. The strength of an aggregate decreases with the saturation, because the force that holds the aggregate together comes principally from the capillary pressure in the saturated pores. As the saturated region recedes into the body, the body expands slightly.

At the same time, differential strain builds up because the solid network is being compressed more in the saturated region than near the drying surface. This can cause warping or cracking in a plate dried from one side, as faster contraction of the wet side makes the plate convex toward the drying side.

#### 2.4 Sintering

Sintering is a process of densification driven by interfacial energy. Material moves by viscous flow or diffusion in such a way as to eliminate porosity thereby reducing the solid-vapor interfacial area. In gels, this area is enormous, so the driving force is great enough to produce sintering at exceptionally low temperatures, where the transport processes are relatively slow. The advantage of gel sintering is complete sintering before crystallization.

Amorphous materials sinter by viscous flow and crystalline materials sinter by diffusion, so the paths along which materials move and the relationship between the rate of transport and the driving force, are quite different. Analysis of viscous sintering is relatively simple in principle, but exact treatments are prevented by the complex geometry of the porous body.

Time-temperature - transformation (TTT) diagrams have long been used by metallurgists to show the influence of thermal history on phase transformation. Uhlmann(1972) introduced this approach as a means of establishing the critical cooling rate needed to produce a glass by quenching a melt. Using standard theories (or measured values) for the rates of crystal nucleation ( $I_v$ ) and linear crystal growth velocity ( $U$ ), the time dependence of the volume fraction ( $V$ ) of crystals produced by a given thermal history can be calculated using

Avrami's equation (Avrami, 1939, 1940, 1941).

$$V = 1 - \exp(- \frac{4}{3} I_v \cdot U^3 \cdot t^4) \sim \frac{4}{3} I_v U^3 t^3$$

(special case of special crystallites)

$I_v$  = nucleation rate

$U$  = linear crystal growth velocity

In this equation the growth and nucleation rates are assumed to be constant, and the crystallites are spherical and isotropic. The approximation applies when the volume crystallized is small. According to the classical theory, the thermal dependence of the nucleation rate (nuclei per unit volume and second) is given by Christian (1975).

$$I_v \propto \exp[-(E_A + E_D)/kT]$$

Where  $E_A$  is the thermodynamic barrier to formation of nuclei and  $E_D$  is the kinetic barrier to diffusion across the liquid-nucleus interface. The crystal growth rate increases with undercooling (i.e., as  $T$  decreases below the liquidus temperature), because the thermodynamic driving force increases; then the rate decreases because of the falling atomic mobility at low temperature, so  $U$  goes through a maximum at temperature  $T_{max}$ . For gels that crystallize rapidly during heating, the transformation will generally be complete before that maximum is reached. Below  $T_{max}$  the crystal growth rate is approximated by

$$r \propto T \cdot \exp(- E_d/k.T)$$

Where  $E_d$  now is the kinetic barrier for transport at the liquid-crystal interface. It is generally assumed that  $E_d$  is equal to the activation energy for viscous flow.

$$V \propto (t/n)^4 \cdot T^3 \cdot \exp(-E_A/k.T)$$

For a spherical nucleus, the thermodynamic barrier is given by

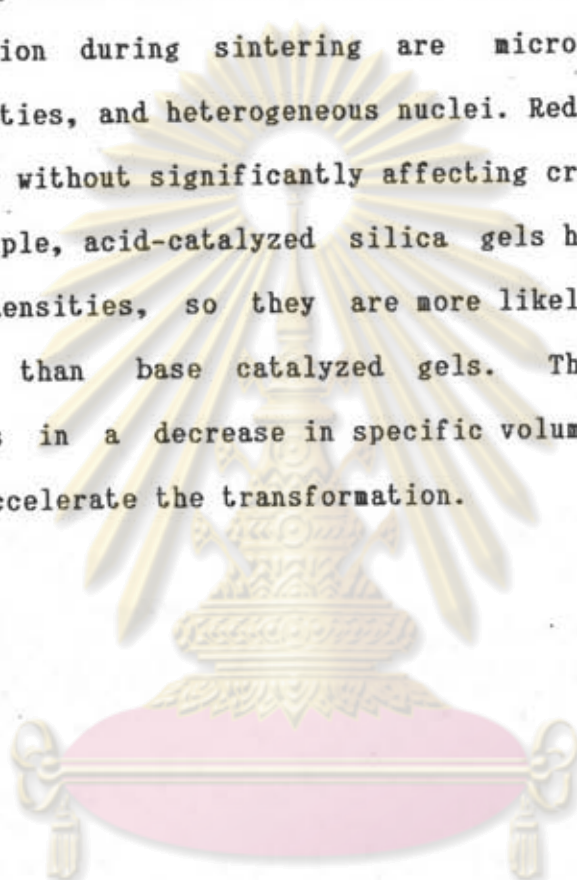
$$E_A = (16\pi/3)\sigma_{SL}^3/(\Delta G_v)^2$$

Where  $\sigma_{SL}$  is the crystal-liquid interfacial energy and  $\Delta G_v$  is the free energy change per unit volume crystallized. Thus the temperature dependence of  $V$  is determined by  $E_A$  and  $\Delta G_v$ .

A typical example of a TTT curve is presented in figure 2.9, where  $I_v$  and  $U$  have been calculated using the viscosity values obtained from sintering studied by Sacks and Tseng (1984), as well as viscosity values for conventional dry silica (i.e., having a low OH content). The curves represent a volume fraction of crystals of  $V = 10^{-6}$ : for times to the left of the curve (e.g., < 10 min. at 1575 K for the "wet" material),  $V < 10^{-6}$ . The viscosity is so much lower in the glass with the high hydroxyl content that the time to reach that degree of crystallization is reduced by ~ 3.5 orders of magnitude. This type of analysis was further extended by Uhlmann, et al. (1986) by combining the transformation curve with densification curves calculated from the theory of viscous sintering. The dashed curves in figure 2.9 represent the time to reach full density at each temperature according to the cylinder model. If the sintering curve does not cross the crystallization curve, then densification can be completed before detectable crystallization occurs. Gels with smaller pores (lower dashed curves) sinter faster, so they are less likely to crystallize before sintering. The crystallization rate does not depend on the microstructure of the gel. So as an important consequence, manipulation of the pore size (e.g., by control of pH

during hydrolysis and condensation) permits decoupling of the rates of transformation and densification. During heating, the amount of sintering depends only on the viscosity-temperature function integrated over the time.

The most important factors that can be used to control the degree of crystallization during sintering are microstructure, applied pressure, impurities, and heterogeneous nuclei. Reducing the pore size speeds sintering without significantly affecting crystal nucleation or growth. For example, acid-catalyzed silica gels have finer pores and higher green densities, so they are more likely to sinter without crystallization than base catalyzed gels. The crystallization usually results in a decrease in specific volume. So, an applied pressure can accelerate the transformation.



ศูนย์วิจัยทรัพยากร  
จุฬาลงกรณ์มหาวิทยาลัย

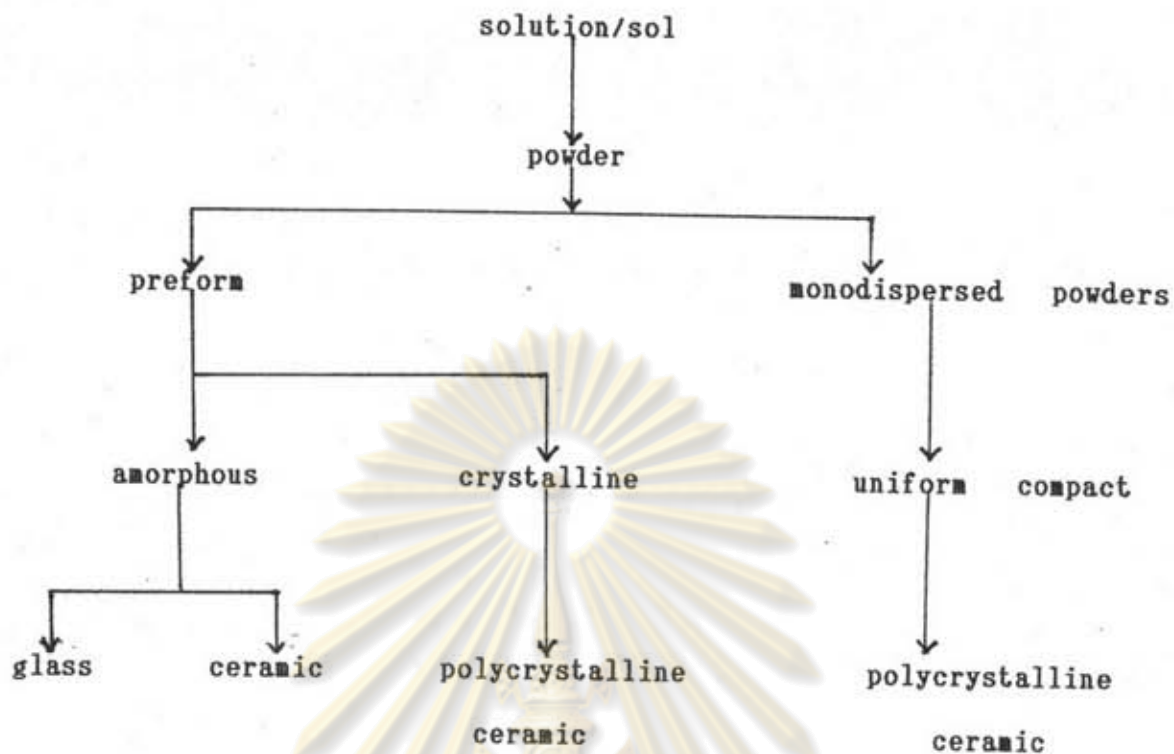


Fig. 2.1: Preparation of glasses, glass-ceramics, and ceramic by the sol-gel process

ศูนย์วิทยทรัพยากร  
จุฬาลงกรณ์มหาวิทยาลัย



Fig. 2.2: Simplified sol-gel process

Table 2.1: Elements used to date in the sol-gel process

Li	Y	Cr	B	N
Na	La	Fe	Al	P
K	Nd	Co	In	As
Cs	Th	Ni	C	Sb
Mg	U	Pd	Si	O
Ca	Ti	Au	Ge	S
Sr	Zr	Zn	Sn	F
Ba	Hf	Cd	Pb	

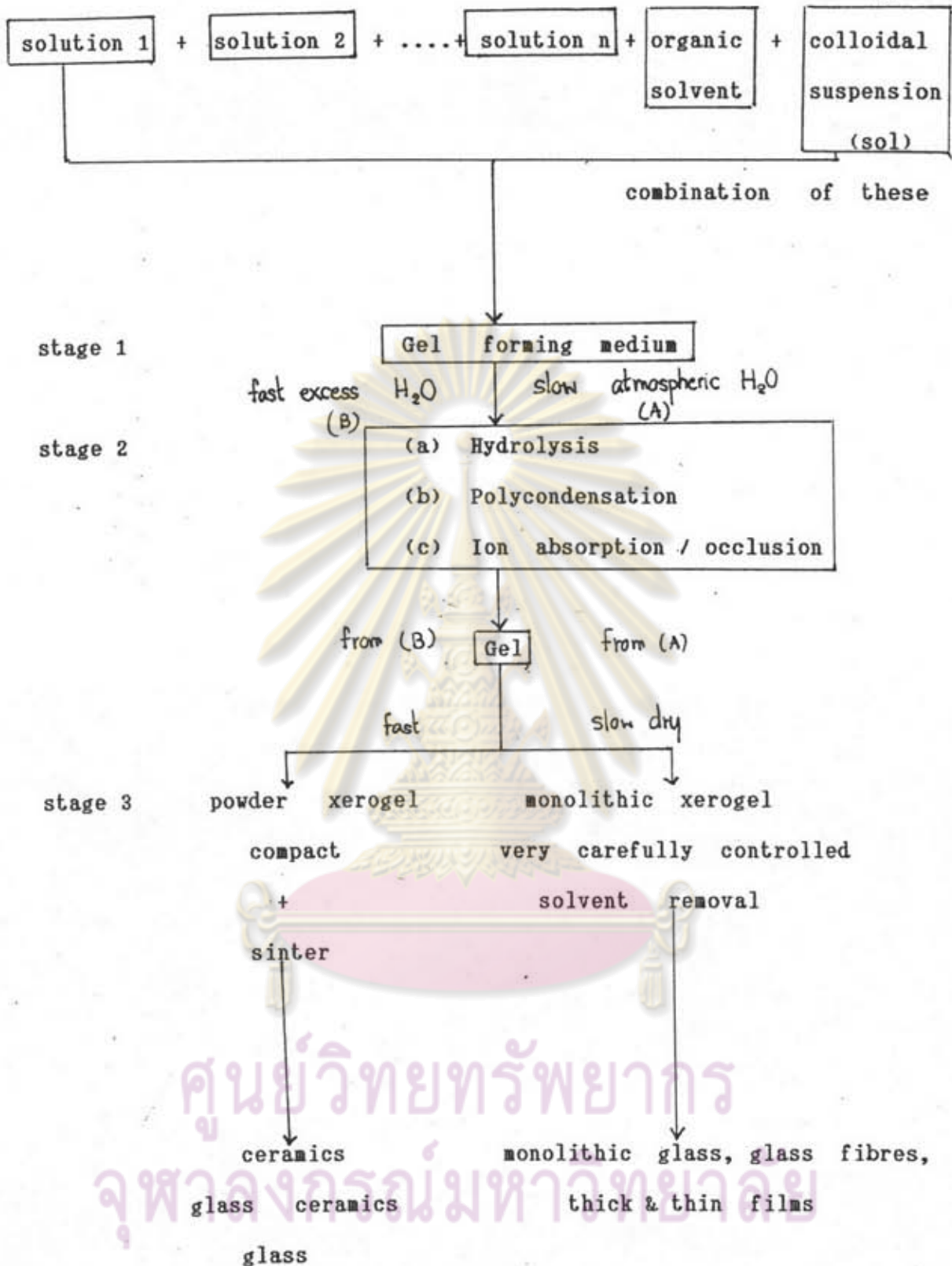


Fig. 2.3 Generalized scheme of sol-gel synthesis



Table 2.2: Point of zero charge (PZC) of selected oxides

Typical Range<sup>a</sup>

Oxide type	PZC
$M_2O$	11.5 < pH
MO	8.5 < pH < 12.5
$M_2O_3$	6.5 < pH < 10.5
$MO_2$	0 < pH < 7.5
$M_2O_5$ , $MO_3$	pH < 0.5

Examples<sup>b</sup>

Oxide type	PZC
MgO	12
FeOOH	6.7
$Fe_2O_3$	8.6
$Al_2O_3$	9.0
$Cr_2O_3$	8.4
$SiO_2$	2.5
$SnO_2$	4.5
$TiO_2$	6.0

<sup>a</sup> from Parks, 1965

<sup>b</sup> selected from Hunter, 1981

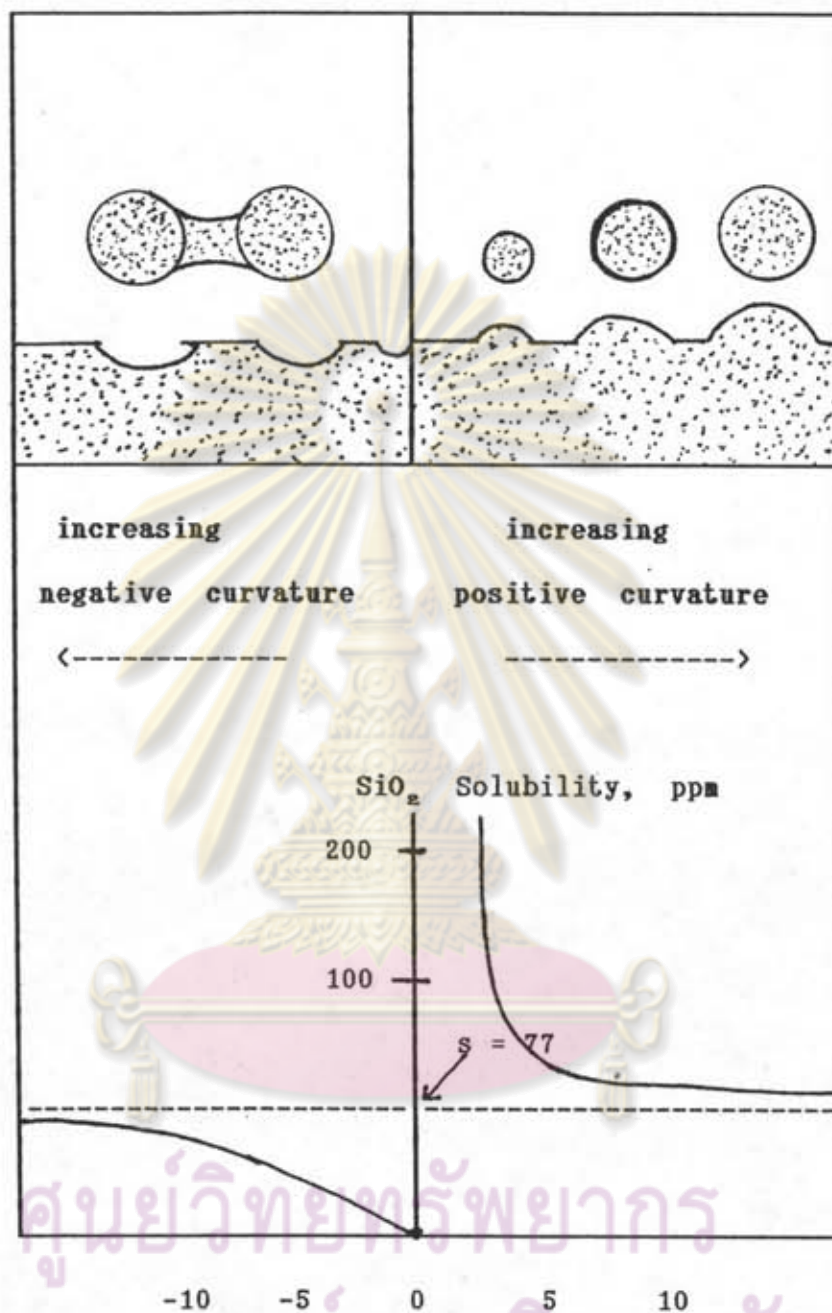


Fig. 2.4: Variation in solubility of silica with radius of curvature of surface. The positive radii of curvature are shown in cross section as particles and projections from a planar surface, negative radii are shown as depression or holes in the surface, from Iler, (1979)

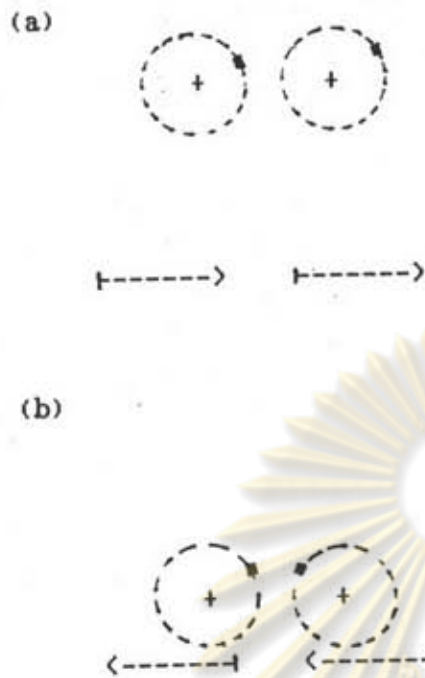


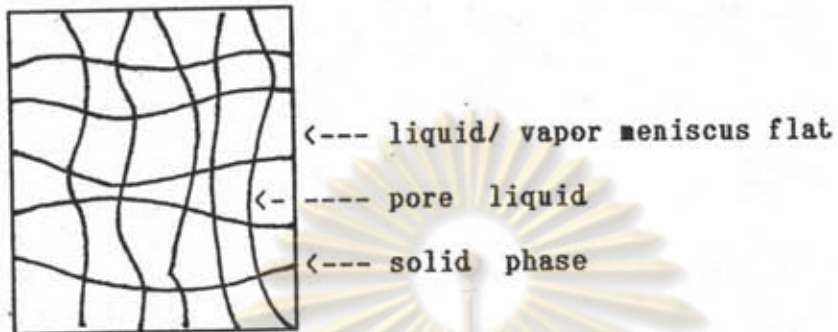
Fig. 2.5: Schematic representation of the origin of the London dispersion forces for two atoms, from Napper, (1983)

	COACERVATES	TACTOIDS	CRYSTALLOIDS	FLOCKS
RODS				
PLATES				
SPHERES				

Fig. 2.6: The principal types of aggregates of rigid colloidal particles, from Heller, (1980)

## Stages of drying

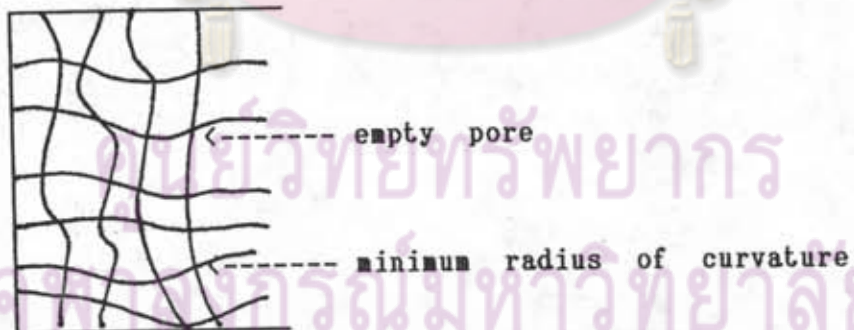
a) Initial condition



b) Constant rate period



c) Falling rate period



maximum capillary pressure

$$P_r = \frac{(\sigma_{sv} - \sigma_{sl}) \cdot sp}{V_p}$$

Fig. 2.7: Schematic illustration of drying process

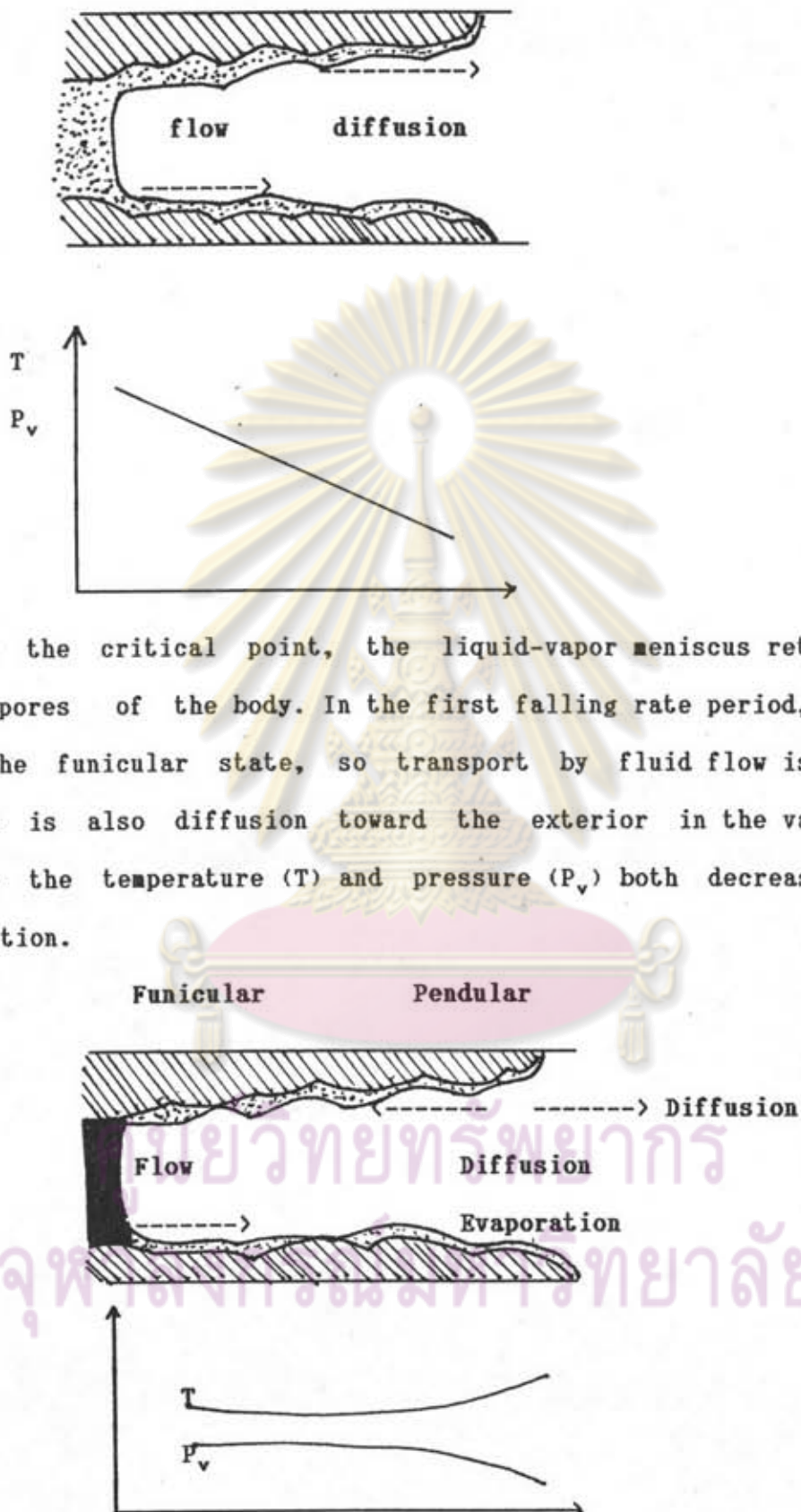
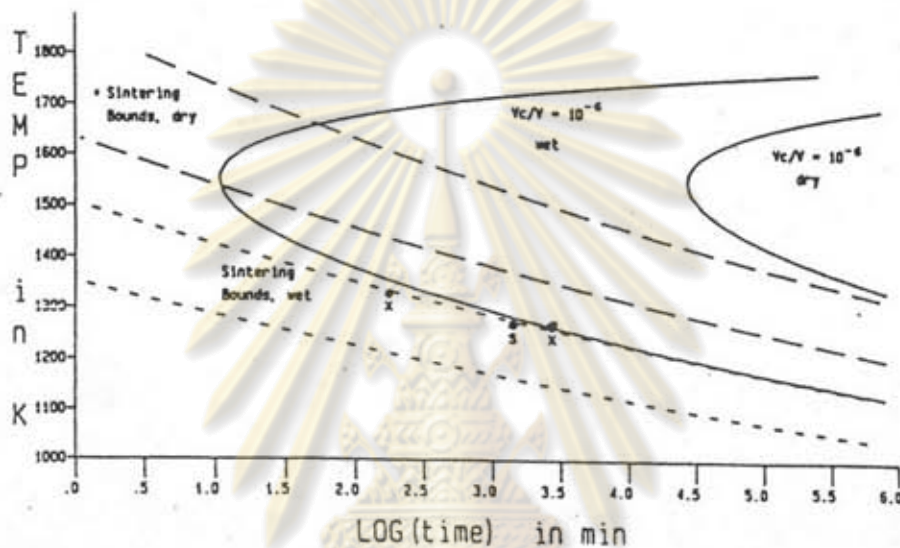


Fig. 2.8 : Schematic illustration of transport during the second falling rate period

Fig. 2.9 : TTT diagram for dry and wet silica, combined with sintering curves



Silica sintering (dashed curves) and crystallization (solid curves) under dry and wet condition; upper and lower sintering bounds correspond to assumed pore diameters of 500 and 5 nm, respectively. The lower viscosity observed by Sacks and Tseng, 1984 shifts all curves to lower times at any temperature. Their data for sol-gel derived glasses are also included: X marks treatments that resulted in crystallization with little sintering and S marks treatments that produced sintered glasses free of crystallinity, from Uhlmann, et al., 1986